CORROSION SCIENCE AND TECHNOLOGY, Vol.5, No.5(2006), pp.153~159

Development of Metallic Bipolar Plate Material with W-addition in Austenitic Stainless Steel for PEMFC Environment

Kwang Min Kim, Sung Ung Koh, and †Kyoo Young Kim

Pohang University of Science and Technology, Pohang 790-784 Korea

Austenitic stainless steels with addition of various amounts of Mo and W were evaluated in terms of corrosion and contact resistance to determine optimum alloy composition of metallic bipolar plate for PEMFC. The corrosion property was evaluated by both acid fume exposure test at 130 ℃ and by electrochemical polarization tests in H_3PO_4 solution at 80 ℃. Austenitic stainless steel with proper amount of Mo and W demonstrated not only good corrosion resistance but also low contact resistance. Analyses on the passive film show that partial substitution of Mo by W enhances passive film stability and repassivation property. Test results suggest that austenitic stainless steel with 2 wt%Mo and 4 wt%W has optimum composition for metallic bipolar plate used in PEMFC.

Keywords *: metallic bipolar plate, PEMFC, W-addition, corrosion, contact resistance*

1. Introduction

The bipolar plates are used in proton exchange membrane fuel cell (PEMFC) to provide the electrical connection between the cells and to supply the inlet reactive gases. On one side of the bipolar plate hydrogen fuel gas for anode is supplied and on the other side oxygen (or air) for cathode is supplied. The material requirements for bipolar plate are high electrical conductivity, good mechanical strength, high chemical stability, and good corrosion resistance. Graphite meets well such materials requirements and it is widely used as bipolar plate material for PEMFC. For commercialization, however, graphite has limitations due to its poor mechanical strength and high cost for machining.[1),2)] Austenitic stainless steel is considered as one of the strong candidate materials due to its excellent mechanical strength and easy machining property.[3),4)] A potential weakness of austenitic stainless steel is corrosion problem by strong acidic electrolyte of PEMFC.[3)] Various modifications for base alloy as well as for alloy surface have been developed to improve corrosion resistance while reducing contact resistance.[5),6)]

PEMFC using the perfluorosulfonic acid (PFSA) polymer membranes (e.g. Nafion) as electrolyte is operated at low temperature, typically 80 ℃. This low operational temperature inherently results in serious technical problems to be solved, including low cathode performance, high material cost for catalysts and low tolerance to fuel impurities, especially CO.[7),8)] PEMFC using a PFSA type electrolyte has limitation to use metallic bipolar plate since metal corrosion contaminates catalysts and decreases efficiency of the cell. High temperature operation of PEMFC can be possible with phosphoric acid (H_3PO_4) electrolyte since it has high thermal stability and high proton conductivity, even in the anhydrous form. PEMFC with H_3PO_4-doped polybenzimidazoles (PBI) membranes can be operated at as high as 200 ℃.[9),10)] Therefore, the key technical issues on gas humidification and CO tolerance can be improved significantly.[11)]

In this study, experimental austenitic stainless steels were prepared with addition of various amounts of Mo and W to determine optimum alloy composition of metallic bipolar plate for PEMFC. The corrosion property was evaluated by both acid fume exposure test 130 ℃ and by electrochemical polarization tests in H_3PO_4 solution at 80 ℃. The contact resistance was measured under various levels of contact force after potentiostatic polarization to form a stable passive layer on the surface. Auger electron spectroscopy was employed to understand the elemental distribution in the passive film and X-ray photoelectron spectroscopy was performed to analyze the chemical state of the elements consisting of the passive film.

†Corresponding author: kykim@postech.ac.kr

Table 1. Nominal composition of experimental stainless steel alloys

Alloy	Mo (wt.%)	W (wt.%)	Alloy	Mo (wt.%)	W (wt.%)
A1	0	0	A5	2	4
A2	2	0	A6	1	6
A3	4	0	A7	0	8
A4	3	2	A8	0	4

2. Experimental procedure

2.1 Specimen preparation and microstructure analysis

The experimental alloys for metallic bipolar plate were prepared from an austenitic stainless steel having a basic composition of 18%Cr-12%Ni-0.02%C-1.5%Mn-0.5%Si-0.03%P-0.003%S-0.2%N. To understand the effects of Mo and W addition on the electrochemical and electrical properties, 8 different alloys were prepared by changing different amount of Mo and W. Table 1 lists nominal compositions of the experimental alloys. The stainless steel ingots were prepared by vacuum induction furnace, and hot rolled to 15 mm thickness. The ingots were homogenized at 1150 ℃ for 15 minutes, followed by water cooling. Microstructure was examined after potentiostatic etching which was performed in an electrolyte containing 10 g oxalic acid in 100 ml H_2O. Potential of 1.8 V_{SCE} (vs. saturated calomel electrode: SCE) was applied for 150 sec.

2.2 Acid fume test

Fig. 1 shows an acid fume tester used in this experiment. Phosphoric acid solution (85% H_3PO_4) was partially filled in a glass cell and the specimen was placed on top of the glass cell using a specimen holder. The acid fume was mixed with H_2 gas and air for anode and cathode environment simulation, respectively. Phosphoric acid was heated to 130 ℃ and the specimen was exposed to hot acid fume for 5 days. Relative severity of acid fume corrosion was evaluated by naked eye observation.

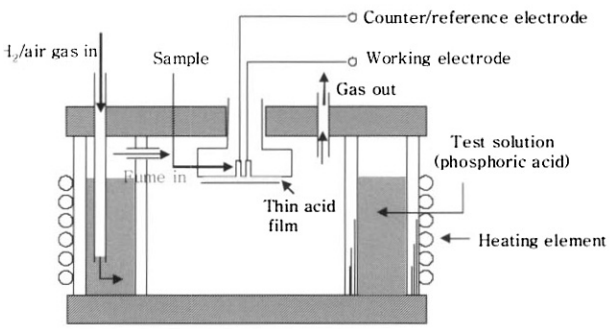

Fig. 1. Schematics of acid fume tester

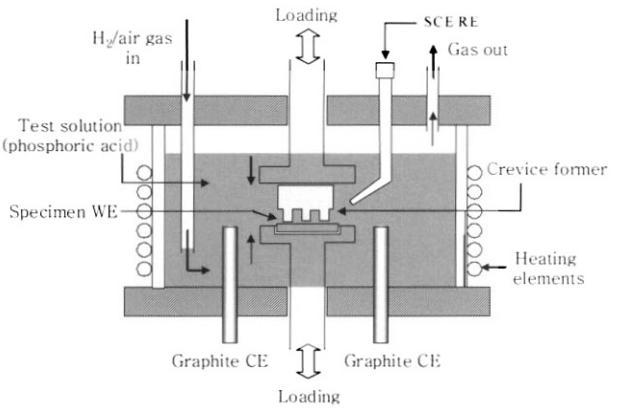

Fig. 2. Schematic diagram of electrochemical test cell

2.3 Electrochemical polarization

Electrochemical polarization tests of both dynamic and static methods were employed to understand the electrochemical property of the experimental alloys in a PEMFC environment. The PEMFC environment used in this experiment was a simulated phosphoric acid type fuel cell electrolyte which contained 0.15 M H_3PO_4. For all electrochemical polarization tests, H_2 gas and O_2 gas were introduced for 1 hour before the start of each set of experiment to simulate anode and cathode environment of fuel cell, respectively. Fig. 2 illustrates the electrochemical cell arrangement used for potentiodynamic and potentiostatic polarization tests. All electrochemical polarization tests were performed at 80 ℃.

For general understanding of electrochemical behavior, potentiodynamic polarization was performed at a scanning rate of 0.5 mV/sec in a potential range of -0.25 V and 1.2 V with respect to the corrosion potential of each steel specimen. Before each potentiodynamic polarization test, oxide possibly present on the specimen electrode was removed by applying -0.7 V_{SCE} for 5 mim, and then potentiodynamic polarization test was set off after maintaining the electrode at an open circuit potential for 5 min.

Potentiostatic polarization tests were performed to examine the formation behavior of passive film and to grow passive layer on the stainless steel for structural analysis of the layer. At applied potentials of -0.1 V_{SCE} for anode simulation and 0.6 V_{SCE} for cathode simulation, the current change was observed with time. To evaluate crevice effect of the steel specimen, potentiostatic polarization tests were performed with the specimen electrode placed in a crevice former. Two types of crevice former were prepared: one was made of Al_2O_3 for examining shear effect of electrolyte on steel and the other was made of graphite for examining galvanic effect between metallic bipolar plate and carbon constituent used in the electrode

assembly of PEMFC. Fig. 2 shows a schematic diagram of electrochemical test cell with crevice former.

2.4 Contact resistance measurement

Contact resistance of the stainless steel specimens was evaluated by measuring voltage value when a current of 2A was applied to two copper end plates between which the stainless steel specimen was located. Compression force was applied from 30 N/cm^2 to 210 N/cm^2 using an Instron 4467.

2.5 Auger spectroscopy and XPS surface analysis

Auger electron spectroscopy (AES) was used to determine the passive film thickness and the elemental distribution in the passive film. Passive film was formed by potentiostatic polarization with an applied potential of 0.6 V_{SCE} for 1 hour in 0.15 M H_3PO_4 solution at 80 ℃ by bubbling air through the solution. After formation of passive film, specimen was washed, rinsed and dried with N_2 gas. Before AES analysis, a special care was given to prevent oxidation of specimen by placing it in N_2 environment. AES was performed with PHI 600 by sputtering with Ar at a rate of 4A°/min on the basis of sputtering Ta_2O_5.

XPS (X-ray photoelectron spectroscopy) was employed to analyze the chemical elements consisting of passive film. To obtain information from both top and bottom parts of the passive film, take-off angles of 30° and 90° were used. Kratos Model XSAM800pci was used with Al Kα source (1486.8eV). Binding energy of the elements was normalized by using binding energy of carbon, 285.6eV.

3. Result and discussion

3.1 Acid fume exposure test

After homogenization treatment, all experimental steels have the same austenitic microstructure with similar grain size and shape. No secondary phase was observed from all the steels. After 5 days of acid fume test at 130 ℃, relative evaluation by naked eye observation was made. Severity of acid fume corrosion was as follows: A1> A2> 3> A7> A8> A4> A5 (A6 were not tested) in air mixed acid fume condition, and A1> A3> A2> A4≈ A5≈ A7≈ A8 (A6 were not tested) in H_2 gas mixed acid fume condition. From acid fume test, it is clearly shown that steels containing W have better corrosion resistance than steels containing Mo alone. In both air and H_2 gas mixed conditions, A5 containing 2 wt%Mo and 4 wt%W seems to have the best corrosion resistance.

3.2 Potentiodynamic polarization

Fig. 3(a) and 3(b) show potentiodynamic polarization behaviors of the experimental steels tested in simulated anode and cathode condition, respectively. General polarization behavior was similar in both anode and cathode conditions. Polarization curves show a large stable passive region and transpassivity near oxygen evolution potential without any sign of pitting corrosion. However, the open-circuit potential (OCP) was more stable in cathode condition than in anode condition. It was due to stability of passive films. The passive film formed in cathode condition with air purging was stable, but not stable in anode condition with H_2 gas purging. The polarization behaviors at -0.1 V in anode condition and at +0.6 V in cathode condition have a significant meaning since PEMFC is operated at these respective overpotentials. At -0.1 V, there was no particular difference in the current density between the different steel samples since no stable passive layer could form at this potential. At +0.6 V, however, a clear difference in passive current was observed from different steel samples since a stable passive layer could form at this high potential. It appears that A5,

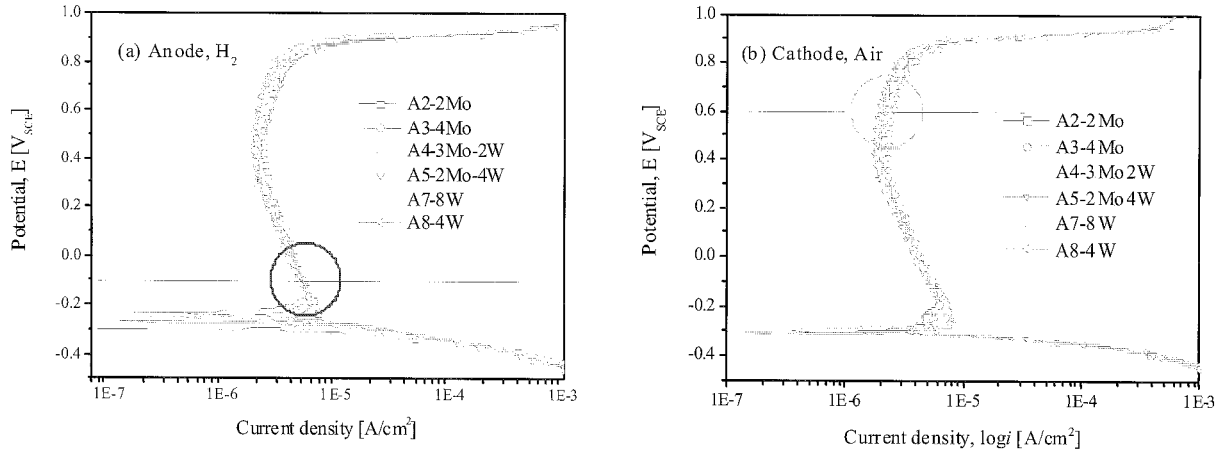

Fig. 3. Results of potentiodynamic polarization test in 0.15M H_3PO_4 solution at 80℃ with H_2 and air.

Table 2. Weight percent of dissolved elements after potentiostatic test (unit: wt.%)

Specimen	Element	Applied Potential (vs.SCE)			
		0.6	0.8	0.9	1.0
A3	Fe	78.2	74.4	64.3	63.0
	Cr	7.4	9.9	17.7	19.1
	Ni	9.9	11.4	14.1	13.9
	Mo	4.5	4.3	3.9	4.0
A5	Fe	78.8	77.4	65.3	64.9
	Cr	8.2	9.4	18.3	18.7
	Ni	10.3	9.4	10.8	11.3
	Mo	2.7	3.8	5.6	5.1
	W	0	0	0	0

A7 and A8 containing W have clearly less passive current density than A2 and A4 containing Mo alone. From both acid fume test and potentiodynamic polarization test, it is clearly shown that addition of W to austenitic stainless steel provides better corrosion resistance in a simulated PEMFC environment.

According to Pourbaix diagram,[12] in acidic solutions of pH less than 4, W presents as insoluble WO_3 in the passive film while Mo presents as a dissolved form of Mo^{3+}. pH value of 0.15 M H_3PO_4 is 1.7. To confirm the insolubility of WO_3, soluble W content for two specimens (A3: 3%Mo vs. A5: 2%Mo-4%W) was measured by ICP after polarizing the stainless steel specimens at potentials above transpassive potential, and the results are listed in Table 2. No soluble W was detected from W-modified steel. This result confirmed that the passive film formed on A5 with W-modification contained insoluble WO_3 which was considered to contribute further increase in passive film stability in acidic environment.

3.3 Potentiostatic polarization with crevice former

The metallic bipolar plate may develop local corrosion depending on design of gas path and operational gas pressure because of complex configuration of gas channels in the plates. To observe local corrosion behavior of experimental steels, potentiostatic polarization test was performed with the specimens placed in a crevice former, as shown in Fig. 2. Two different materials were used for crevice former; one was Al_2O_3 for initiation of crevice corrosion due to simple geometric effect and the other was graphite for initiation of crevice corrosion due to combined effect of geometry and galvanic coupling. Galvanic corrosion is possible between the metallic bipolar plate and gas-diffuse carbon constituents used in PEMFC. Potentiostatic polarization test was performed mainly with two experimental steels of A3 with Mo alone and A5 with Mo and W. All potentiostatic polarization tests were performed using 0.15 M H_3PO_4 solution at 80 ℃. For cathode environment, 0.6 V_{SCE} was applied with air purging and for anode environment -0.1 V_{SCE} was applied with H_2 gas purging.

Before using crevice former, a simple potentiostatic polarization test was performed to observe a shear electrochemical effect of the electrolyte on the local corrosion property of the steels during long term operation of PEMFC. In all cases, after significant initial drop within 30 min, current decreases gradually and reaches a stable steady state value. Even though a transient pitting was observed from A3 in anodic condition after about 1000 sec, it disappeared and stabilized thereafter. Between anode and cathode conditions, the current value was lower in cathode condition than in anodic condition. In both anode and cathode conditions, A5 containing W showed lower current value than A3 containing Mo addition. With Al_2O_3 and graphite crevice former, potentiostatic polarization test results were quite similar except more frequent and higher transient pitting peaks in air-purged cathode condition with graphite crevice former than those with Al_2O_3 crevice former. However, no transient pitting peaks were observed from both steels tested in H_2 gas-purged anode condition.

Fig. 4 shows a typical potentiostatic polarization test result of A3 and A5 placed in graphite crevice former in a simulated air-purged cathode condition with applied potential of 0.6 V_{SCE}. The current values of A5 containing W were lower than those of A3 containing Mo alone. Transient current peaks were observed initially from both steels and eventually disappeared after about 3000 se

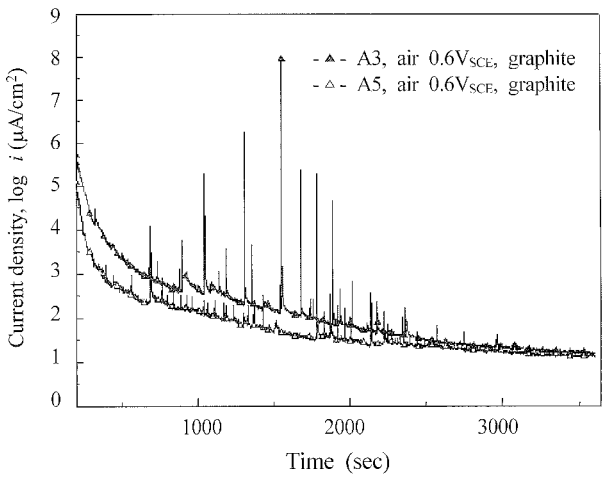

Fig. 4. Result of potentiostatic test in 0.15M H_3PO_4 solution at 80℃ with graphite crevice former in air-purged cathode environment.

conds. A5 showed much lower peak current density than A3. Comparing to the transient peaks observed with Al_2O_3 crevice former in the same cathode environment, frequency of transient peak occurrence and overall current values increased significantly. However, increase in overall current values was simply due to increase in the surface area by galvanic coupling which means that both areas of specimen and graphite crevice former acted as working electrode. This comparison suggests two factors. One is that galvanic coupling between the metallic bipolar plate and carbon constituent used in the electrode assembly of PEMFC may lead to crevice corrosion. Another is that once crevice corrosion occurs, then it can be quite serious if a proper material is not selected.

Examination on the potentiostatic polarization test results clearly shows that the overall current and peak current values of A5 are lower than those of A3. This can be explained by passive film stability and repassivation characteristics. The effect of W on passive film stability and repassivation rate has been well studied previously.[13),14)] It has been reported that the beneficial effect of W is due to the interaction of tungsten oxide (WO_3) with oxides of Cr and Fe, resulting in enhanced stability and enhanced bonding of the oxide layers to the base metal. Thus, partial substitution of Mo by W can improve effectively the resistance of local corrosion of stainless steel bipolar plate in PEMFC environment.

3.4 Contact resistance measurement

Fig. 5 shows the contact resistance test results for the experimental steels with various amounts of Mo and W. For contact resistance test, passive films were grown for 1 hour in a simulated air-purged cathode condition. The contact resistance test was performed with applied pressure up to 210 N/cm^2 which was known as typical contact pressure applied to bipolar plate in PEMFC.[3)] The contact resistance under 210 N/cm^2 decreased in the order of A4> A3> A8 ≈ A5>A7. This result clearly shows that the contact resistance decreases with increasing W content in austenitic stainless steel. This is very exciting result since the steels containing high W show not only better corrosion resistance but also lower contact resistance than the ones containing Mo alone. The main materials requirement of metallic bipolar plate is high corrosion resistance and low contact resistance.

To determine optimum composition of Mo and W content, it is necessary to evaluate overall performance of electrochemical property and contact resistance. Fig. 6 compares test results of passive current density and contact resistance. From this comparison, it is shown that A5 has best corrosion resistance while A7 has the lowest contact

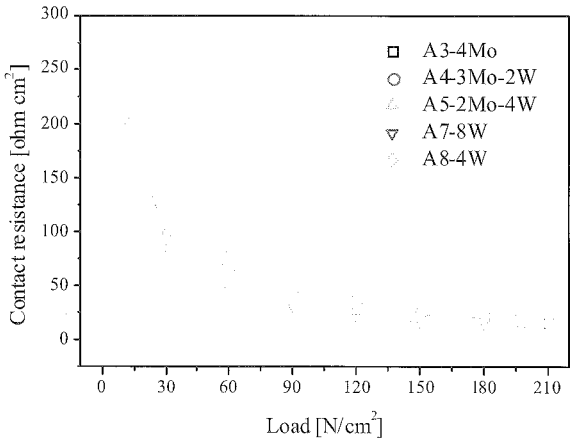

Fig. 5. Contact resistance measured at various contact pressures after postentiostatic polarization test in air-purged cathode environment.

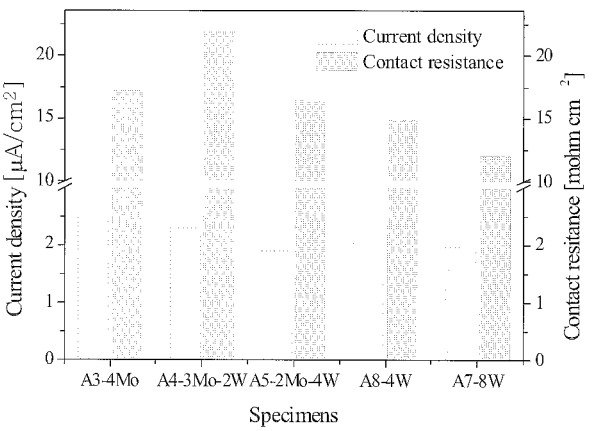

Fig. 6. Comparison of overall performance of the experimental steels with various Mo and W content.

resistance. However, A7 containing 8 wt%W may have a difficulty in steel making process, particularly during hot rolling since metallurgical defects are expected due to formation of second phase precipitation such as σ phase. Considering all these factors of corrosion resistance, contact resistance and steel making process, A5 having 2 wt%Mo and 4 wt%W would be an optimum composition for austenitic stainless steel bipolar plate.

3.5 AES and XPS analysis

XPS analysis was performed to understand the chemical state of the elements consisting of the passive film. Using take-off angles of 30° and 90°, information on top and bottom of the passive layer was obtained. Regardless of steel composition, Cr in the passive layer presents in the form of Cr, Cr_2O_3, $Cr(OH)_3$, CrO_3, and CrO_4^{2-}, while Mo in the form of Mo, MoO_2, $MoO(OH)_2$, MoO_3, and MoO_4^{2-}. Comparison of peak area of the main spectra of Cr and

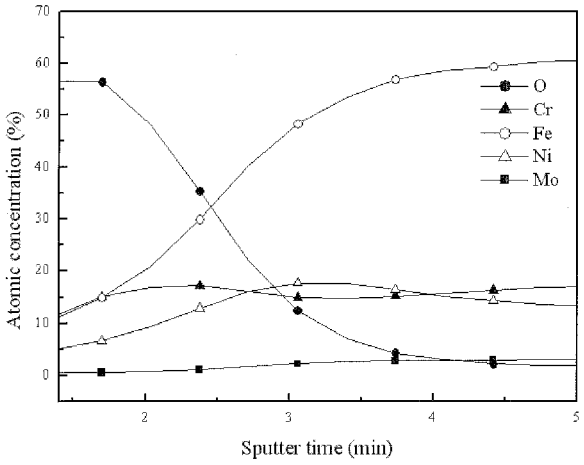

(a)

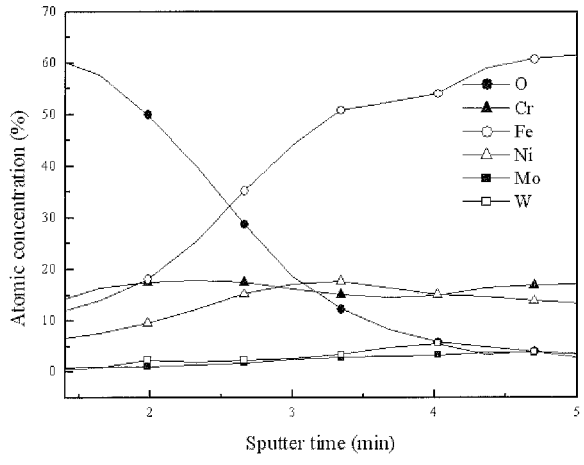

(b)

Fig. 7. AES depth profile on the surface of steel specimen after passivation for 2 hours in H_3PO_4 solution at 80℃; (a) for A3 steel and (b) for A5 steel.

Mo between A3 and A5 suggests that addition of W increases the ratio of Cr_2O_3/ $Cr(OH)_3$ and enhances concentration of MoO_4^{2-}. XPS results indicates that contribution of W for corrosion resistance is stabilization of passive film by enhancing stable Cr_2O_3 and by increasing concentration of MoO_4^{2-} which has a cation selectivity.

AES analysis was performed on A3 and A5 to understand elemental distribution along the passive film. Fig. 7 shows elemental distribution along the passive film from the surface to substrate. In both steels, Cr profile shows that Cr concentration decreases near the interface between the passive layer and substrate but enriched inside the passive film. On the other hand, Ni enriches in the interface region between the passive film and substrate. However, for A5 containing W, W profile indicates that W is enriched in the interface region between the passive film and substrate. The main element of Fe shows gradual decrease toward the surface with no enrichment in any particular region. Comparison of the elemental distribution profile between A3 and A5 suggests that addition of W does not affect concentration and distribution of Fe, Ni and Mo, but definitely affects concentration and distribution of Cr and O. Cr profile between A3 and A5 indicates that addition of W not only enhances concentration of Cr in the Cr enriched region but also broadens the Cr enriched region. Addition of W also extends the oxygen profile more toward the substrate. The effect of W addition on both Cr and O profile suggests thickness of the passive film layer can be influenced by the presence of W in the alloy. Thickness of passive film, which was formed after passivation for 2 hours in H_3PO_4 solution in air-purged cathode condition with applied potential of +0.6 V_{SCE} at 80 ℃, was 1.8 nm for A3 containing Mo alone and 2.4 nm for A5 containing Mo and W. This means that A5 containing W with thicker passive film has lower contact resistance. This characteristic is highly desirable one to develop a metallic bipolar plate for PEMFC. However, this new observation can not be explained clearly since currently the effect of W-modification on conduction mechanism of the passive film is not well understood. One possible way of explanation is that high conducting WO_3 makes a complex oxide with both γ-Fe_2O_3 and Cr_2O_3 in the passive layer. The conductivity is $1.2\times10^{-5}\Omega^{-1}$ for WO_3 and $3.0\times10^{-7}\Omega^{-1}$ for MoO_3 at 80 ℃ and $6.0\times10^{-6}\Omega^{-1}$ for WO_3 and $6.0\times10^{-8}\Omega^{-1}$ for MoO_3 at 25 ℃.[15),16)] The conductivity of WO_3 is almost 2 orders of magnitude higher than that of MoO_3. A further study on the effect of W addition on the electronic structure of passive film is required to understand clearly the high conductive nature of the passive film formed on austenitic stainless steel containing W.

4. Summary

Austenitic stainless steels with addition of various amounts of Mo and W were evaluated in a simulated H_3PO_4 type PEMFC environment to determine optimum alloy composition of metallic bipolar plate. The results can be summarized as follows:

1. Corrosion test results of acid fume exposure and potentiodynamic polarization show that austenitic stainless steels containing W have less acid fume attack and better passive film stability than the ones containing Mo alone.

2. Potentiostatic polarization test results with various crevice formers suggest that crevice corrosion may not be a problem for the austenitic stainless steel containing W during long term exposure to PEMFC environment.

3. The contact resistance of the austenitic stainless steel can be reduced by alloying with a proper amount of Mo and W.

5. Overall examination of the test results suggests that the austenitic stainless steel containing 2 wt%Mo and 4 wt%W would be a recommended alloy composition for metallic bipolar plate material used in PEMFC.

Acknowledgments

This work was partially supported by POSTECH research fund and by Samsung Advanced Institute of Technology.

References

1. D. P. Davies, P. L. Adcock, M. Turpin, and S. J. Rowen, *J. Power Sources*, **86**, 237 (2000).
2. T. Besmann, J, Henry, and J. Klett, *Proc. Fuel Cell Seminar*, p. 61 (2003)
3. H. Wang, M. A. Sweikart, and J. A. Turner, *J. Power Sources*, **115**, 243 (2003).
4. S. Lee, J. Lai, and C. Huang, *J. Power Sources*, **145**, 362 (2005).
5. E. Cho, U. Jeon, S. Hong, I. Oh, and S. Kang, *J. Power Sources*, **142**, 177 (2005).
6. J. Scholta, B. Rohland, V. Trapp, and U. Foken, *J. Power Sources*, **84**, 231 (1999).
7. Q. Li, R. He, O. J. Jensen, and N. J. Bjerrum, *Chemistry of Materials*, **15**, 4896 (2003).
8. P. Costamagna and S. Srinivasan, *J. Power Sources*, **102**, 242 (2001).
9. J. S. Wainright, J.-T. Wang, D. Weng, R. F. Savinell M. Litt, *J. Electrochem. Soc.*, **142**, L121 (1995).
10. J. S. Wainright, M. Litt., and R. F. Svinell in *Handbood of Fuel Cells*, Vol. 3, Eds. W. Vielstich, A. Lamm and H. A. Gasteiger, John Wiley & Sons Ltd., p. 436 (2003)
11. Q. Li, R. He, J. O. Jensen, and N. J. Bjerrum, *Fuel Cells*, **4**, 147 (2004).
12. M. Pourbaix, *Atlas of Electrochemical Equilibria in Aqueous Solution*, NACE, Huston, 1974
13. A. Belefrough, C. Masson, D. Vouagner, A. M. De Becdelivre, N. S. Prkash, and J. P. Audouard, *Corros. Sci.*, **38**, 1639 (1996).
14. J. S. Kim, P. J. Xiang, and K. Y. Kim, *Corrosion*, **61**, 174 (2005).
15. D. Manno, M. Di. Giulio, A. Serra, T. Siciliano, and G. Micocci, *J. Phys. D: Appl. Phys.*, **35**, 228 (2002).
16. M. Di. Giulio, D. Manno, G. Micocci, A. Serra, and A. Tepore, *J. Phys. D: Appl. Phys.*, **30**, 3211 (1997).